

Autooxidation of Simvastatin

George B. Smith*, Lisa DiMichele*, Lawrence F. Colwell, Jr., George C. Dezeny,
Alan W. Douglas, Robert A. Reamer, and Thomas R. Verhoeven

Department of Process Research, Merck Research Laboratories
Division of Merck & Co., Inc.
P.O. Box 2000, Rahway, New Jersey 07065, USA

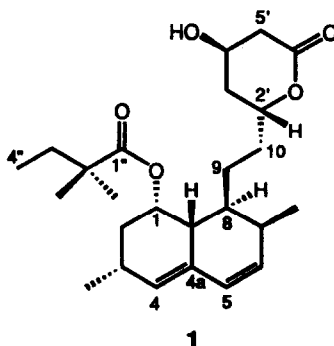
(Received in USA 8 March 1993)

Abstract Autooxidation of the cholesterol-lowering agent simvastatin in ethylene dichloride solution with an azo-type free-radical initiator was investigated in kinetic studies using HPLC. The primary products were oligomers, with peroxide groups within the backbone chain, and some monomeric epoxides. These and several secondary products were isolated chromatographically and identified spectroscopically. A reaction scheme was proposed in which the oligomers arise from competitive hydrogen abstraction and addition reactions of oligomeric free radicals with simvastatin while the epoxides arise from homolytic peroxide cleavage.

INTRODUCTION

The fact that oxygen copolymerizes with various monomers in free-radical polymerizations has been known for many years,^{1,2} but only in more recent times have such polymeric peroxides been studied in detail.³ Cais and Bovey,⁴ the first to study a polyperoxide using NMR, elucidated the structure of polystyrene peroxide and showed that copolymerization produced an equimolar copolymer with a molecular weight of 8000 as measured by light-scattering techniques. Earlier work in this field has been reviewed by Mayo.⁵ Polystyrene peroxides were made by Nukui *et al.*⁶ by copolymerizing styrene and oxygen in the presence of cobalt (II) Schiff bases as oxygen carriers. More recently, alkyl peroxides were characterized using NMR, IR and Raman spectroscopy.⁷ The product mixtures from autooxidations of several 1,3-dienes to oligomers, with peroxide groups within the backbone chain, were studied using gel permeation chromatography and NMR spectroscopy.⁸

Simvastatin **1** is widely used to treat hypercholesterolemia. The molecule is susceptible to slow oxidative degradation which is avoided during synthesis and storage using an inert atmosphere. The present study was undertaken in order to gain insight into the complex autooxidation of **1** in solution.



Compound **1** was aerated in ethylene dichloride solution, avoiding lactone ring opening that might occur in protic media. In the absence of a free-radical initiator the autooxidation was relatively slow at first and accelerated gradually. The induction was eliminated using an initiator, and quantitation of the rates of disappearance of **1** and appearance of the products was easier. The course of the autooxidation, however, was the same in complete detail as viewed using HPLC. All of the same products formed in the same relative amounts, and no new products were evident. The initiator was 2,2'-azobis(4-methoxy-2,4-dimethylvaleronitrile), hereafter called AMDN.

Oligomers with peroxide linkages and some monomeric epoxides formed from **1**. The appearance of these primary products and others derived from them was monitored in kinetic runs using HPLC with diode array detection. The products were isolated using HPLC and identified using NMR, UV and mass spectrometry.

IDENTIFICATION OF THE AUTOOXIDATION PRODUCTS

The products exhibiting sizable HPLC peaks were observed by monitoring three wavelengths simultaneously with HPLC system I and one of those wavelengths with a more polar system II (see Experimental Section); no additional peaks were evident at other wavelengths. Chromatograms of an autooxidation mixture at 50% conversion of **1** are shown in Figures 1 and 2, in which the peaks are labeled with the numbers of the primary products shown in schemes I-III and the secondary products in scheme IV. The structures were determined using ^1H and ^{13}C NMR. Assignments are presented in the footnotes for the products and the starting material **19** for comparison. Further support for the structures of these primary and secondary products was obtained from UV and MS data summarized in Tables I and II.

The autooxidation mixture was dominated by a series of oligomers, whose monomer was identified by NMR as the hydroperoxide **2**.¹⁰ The ^{13}C spectrum showed a resonance at 83.4 ppm diagnostic for a hydroperoxyl group at the C_6 carbon.⁷ This assignment was supported by a low field (9.47 ppm) signal in the ^1H spectrum. The H_6 proton shift (4.19 ppm) was similar to that of a hydroxyl-bearing methine; however, its correlation to the C_6 carbon in a heteronuclear shift-correlated (HETCOR)¹¹ 2-D NMR experiment clearly distinguished it. The α -stereochemistry of the 6-hydroperoxyl group was determined via NOE (nuclear Overhauser effect) difference spectroscopy. Irradiation of the 7-methyl group showed 4% NOE enhancement to H_6 as indicated in scheme II. An observed vicinal coupling ($J_{5,6} = 5.2$ Hz) further supported this stereochemistry. The FAB mass spectrum of **2** revealed the MH^+ parent ion (m/z 451) and included strong $[\text{MH}-16]^+$ and $[\text{MH}-18]^+$ signals indicating losses of oxygen and water. Upon spiking with lithium acetate, the $[\text{M}+\text{Li}]^+$ ion (m/z 457) was observed along with the $[\text{M}+\text{Li}-16]^+$ ion.

The identity of hydroperoxide **2** was confirmed by its clean sodium borohydride reduction¹² to the corresponding 6-alcohol **10**^{13a,13b} (see Experimental Section), whose C_6 signal in the ^{13}C spectrum exhibited a 13 ppm upfield shift to 70.4 ppm. The 6-OH was observed at 1.31 ppm in the ^1H spectrum. The FAB spectrum of **10** indicated loss of water with no evidence of the parent ion. Upon spiking with lithium acetate, however, the signal of the $[\text{M}+\text{Li}]^+$ ion (m/z 441) was observed. More rigorous treatment of **2** with lithium borohydride produced **11**,¹⁴ whose ^1H spectrum showed well resolved signals ascribed to the five hydroxyl groups. The integrity of the stereochemistry at C_6 was maintained in both **10** and **11**.

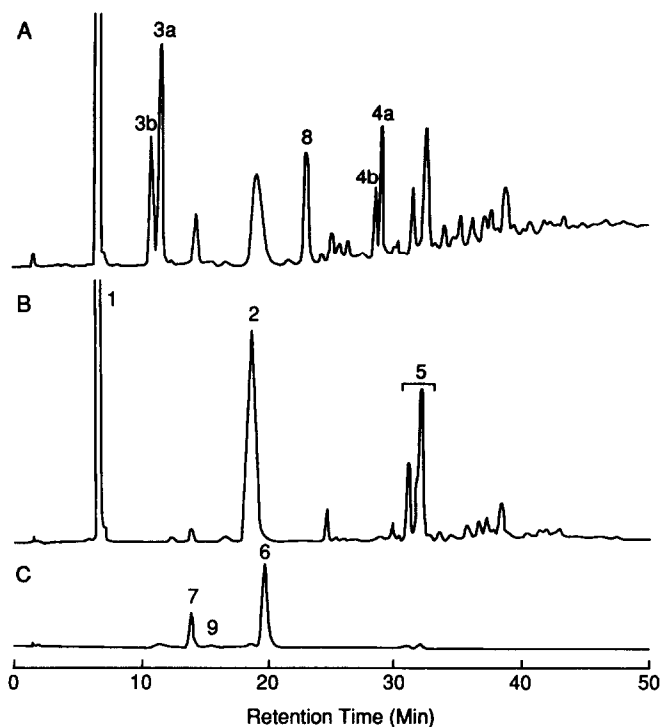


Figure 1. System I chromatograms of an autooxidation mixture with initial concentrations 50 mM **1** and 0.6 mM AMDN, after 6 h at 35°, monitored at 210 nm and 200 maufs (A), at 242 nm and 500 maufs (B), and at 290 nm and 200 maufs (C).

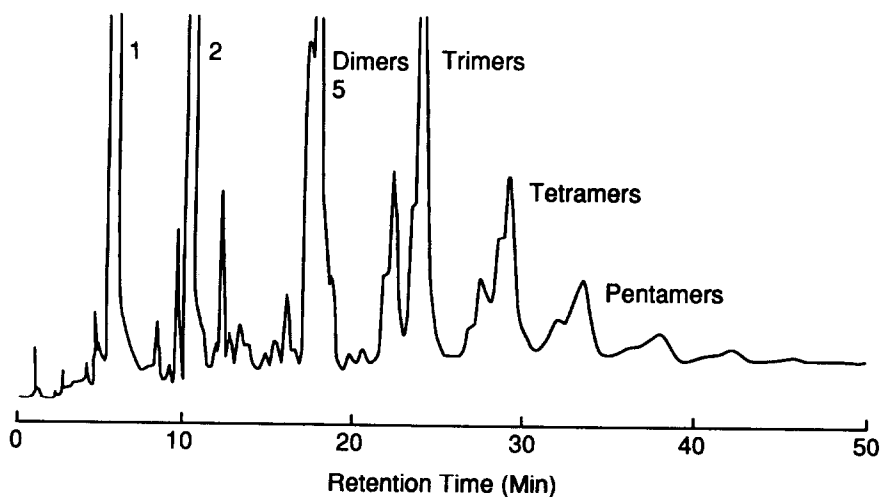
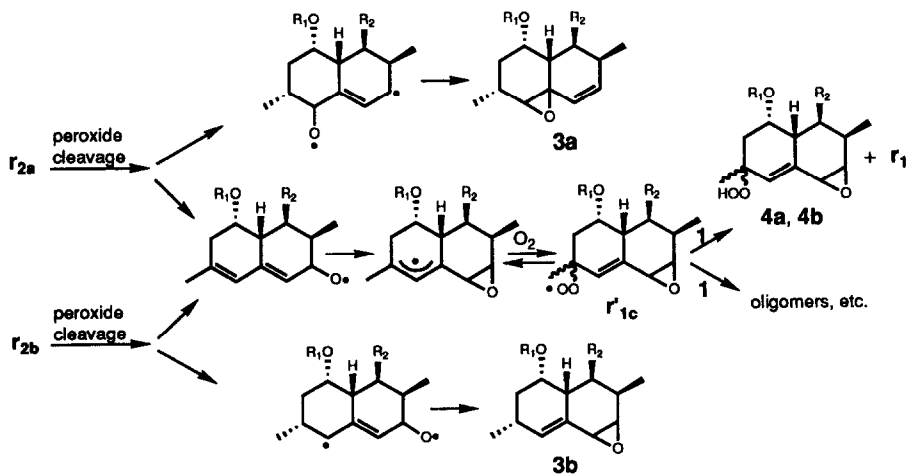
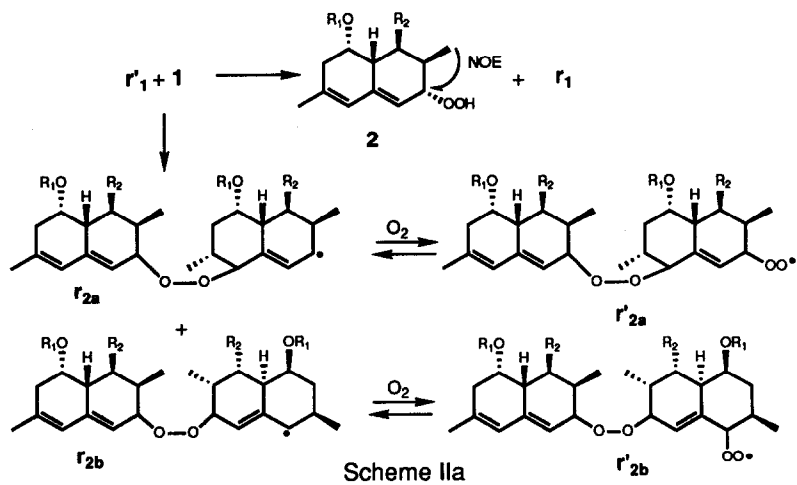
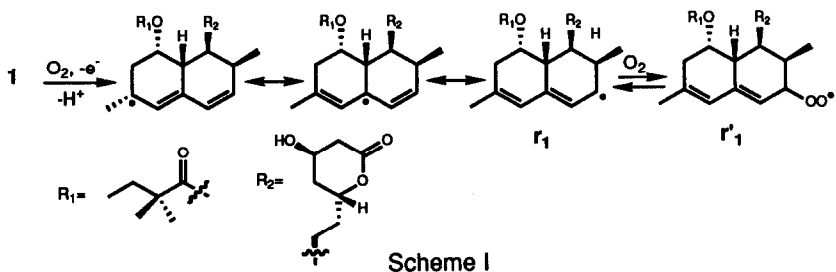
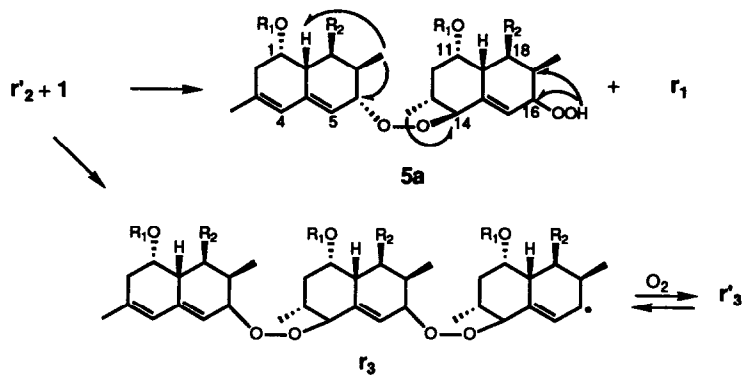
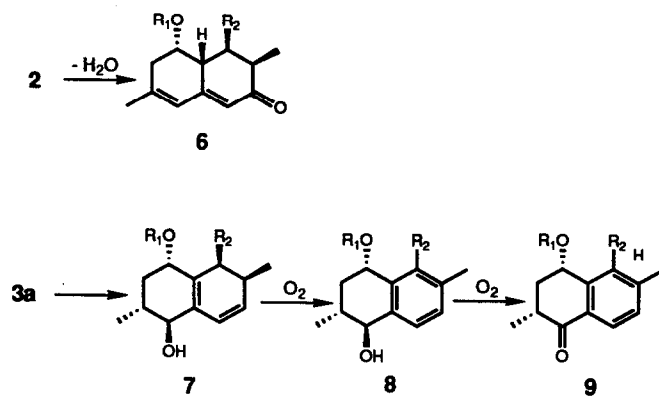


Figure 2. System II chromatogram of an autooxidation mixture with initial concentrations 50 mM **1** and 0.6 mM AMDN, after 6 h at 35°, monitored at 242 nm.





Scheme III



Scheme IV

Table I. Correlation of HPLC Peaks, Structures and UV Spectra

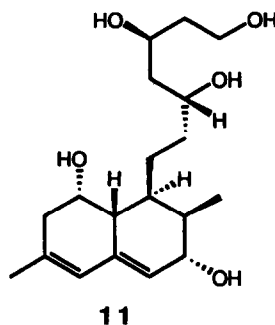
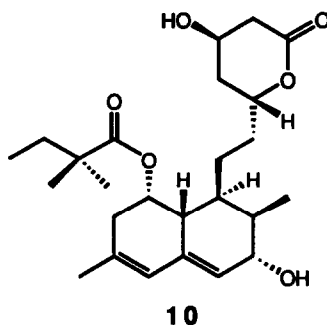
Retention Time, min ^a	Structure	Absorbance (λ_{max} , nm)
4	AMDN	b
7	1	238
11	3b	c
12	3a	c
14	7	255
15	9	265
19	2	242
20	6	290
23	8	215 ^d
28	4b	c
29	4a	c
31	5b ^e	242
32	5a	242

^a HPLC system I. ^b Weak end absorbance only. ^c End absorbance only.

^d Inflection. ^e Isomer of 5a.

Table II. High Resolution Exact Mass Data

Compound(s)	Empirical Formula	Calculated MW	Found MW
2	C ₂₅ H ₃₈ O ₇	450.2217	450.2220
3a + 3b	C ₂₅ H ₃₈ O ₆	434.2668	434.2667
4a + 4b	C ₂₅ H ₃₈ O ₈	466.2166	466.2159
5a	C ₅₀ H ₇₆ O ₁₄	900.4531	900.4508
10	C ₂₅ H ₃₈ O ₆	434.2668	434.2671



The oligomers were observed, using HPLC system II (Figure 2), as regularly spaced groups of partially resolved peaks. Three components of the group 5 eluting immediately after the monomer 2 were resolved and isolated using modified HPLC and identified as dimers. Each of their FAB spectra indicated a molecular weight of 900 daltons, exactly twice the weight of 2. All three, like 2, exhibited an UV absorbance maximum at 242 nm characteristic of the 3,4a-dienes.

The peak areas of the three resolved dimers, monitored at 242 nm, indicated a 10:3:1 ratio. Only the largest component was isolated in sufficient quantity for NMR characterization. It was identified as 5a,¹⁵ the

dimer shown in scheme III. NOE difference experiments were used to establish the regiochemistry of the hydroperoxide at C₁₆ and the α - and β -stereochemistry of the peroxy linkage at C₆ and C₁₄ respectively. The observed NOEs are represented by curved arrows in scheme III. Irradiation of the low field hydroperoxide proton showed NOE enhancement to H₁₆ and H₁₇. NOEs were observed to H_{8a} and H₆ when the 7-CH₃ was irradiated. The α -stereochemistry of H₁₄ was defined by its NOE enhancement from the irradiated 13-CH₃.

FAB spectra of the next three regularly spaced groups of HPLC peaks after the dimers, in order of elution, showed molecular weights consistent with trimers, tetramers and pentamers of 2. The spectrum of each group, like those of the dimers, indicated the [M+Li]⁺ parent ion and more intense ions representing losses of a single water and one or more oxygen atoms. The water might come from the terminal hydroperoxyl group. The number of oxygen-loss ions equaled the number of peroxide linkages in the molecule as if partial loss of oxygen occurred at each linkage. Fragments indicating homolytic cleavage of the peroxide linkage were observed also. Negative-ion FAB spectra included weak [M-H]⁻ ions and fragmentation patterns corresponding to those observed under positive FAB conditions.

Epoxides 3a and 3b¹⁶ were formed in the autooxidation of 1 in a 2.3:1 ratio (based on integrals measured in the ¹H NMR spectrum of the isolated mixture). The ¹H resonances assigned to H₄ (d_H=2.97) in 3a and H₅, H₆ (d_H= 3.35, 3.28) in 3b are characteristic of epoxide.¹⁷ Diagnostic CH coupling constants, derived from a ¹H coupled ¹³C spectrum, were observed for the epoxide carbons C₄ (J=177.4 Hz) in 3a and for C₅, C₆ (J=176.8, 177.4) in 3b and are consistent with the literature.¹⁸ The oxidation of 1 to form these epoxides was confirmed chemically by treatment of 1 with *m*-chloroperbenzoic acid (see Experimental Section) which yielded 3a and 3b in a similar ratio.

Closely related to the 5,6 epoxide 3b were the epimers 4a and 4b,¹⁹ formed in a 2:1 ratio and unresolved by HPLC. The hydroperoxyl groups at C₃ gave rise to low field active hydrogens at 7.53 and 7.65 ppm in the ¹H spectrum and ¹³C shifts of 81.0 ppm for the major 4a and 79.8 ppm for the minor 4b. A tentative assignment of stereochemistry at C₃, where 4a and 4b are the α - and β -CH₃ isomers, respectively, is based on NOEDS experiments.

The remaining numbered HPLC peaks in Figure 1 are those of secondary autooxidation products, which exhibited unique UV spectra; see scheme IV and Table I. Dienone 6²⁰ was chromatographically and spectroscopically identical to authentic material whose structure has been published.²¹ Compound 7,²² isolated in very small quantity, was characterized by ¹H NMR only. The regiochemistry of its double bonds and 4-OH group is based on a homonuclear shift-correlated (COSY²³) 2-D NMR experiment. The equatorial orientation of the 4-OH is based on the J_{3,4} coupling of 7.2 Hz, consistent with diaxial H₃ and H₄ protons. The ¹H spectrum of 8²⁴ showed low field resonances at 7.28 and 7.19 ppm for H₅ and H₆ respectively, compared to the spectrum of 7 (d_H=5.57, 6.16) which indicated that the B-ring of the decalin system in 8 was aromatized. This was further supported by 1-D ¹³C, COSY and HETCOR data. Oxidation of 8 yields the ketone 9.²⁵ The influence of the carbonyl at C₄ is reflected in the 0.6 ppm lower field shift of H₅ (d_H=7.90) compared to that of 8.

RESULTS AND DISCUSSION

HPLC responses were determined for 2, a mixture of 3a and 3b, another of 4a and 4b, and 5a, isolated from the autooxidation mixture, in order to estimate the yields from peak area kinetic data. The molar

response of 2 (or 5a) at 242 nm was used for all of the oligomers, assuming that each is composed of a single common diene unit ($\lambda_{\text{max}} = 242 \text{ nm}$) and the rest monoene units absorbing only at lower wavelengths. Reference standard 6 was used,²¹ and the responses of 7, 8 and 9 were estimated using ergosterol, 1-tetralol and 1-tetralone as reference materials.

Starting material disappearing in autooxidations with initial concentrations of 1 from 10 to 100 mM was found accountable in terms of the observed products. The kinetic data for 1 shown in Figure 3, for example, agree with the sum of the product yields indicated in Figures 4, 5 and 6. (Chromatograms of the same autooxidation mixture are shown in Figures 1 and 2.) Thus all of the significant products seemed to be in view.

The autooxidation of 1 is thought to stem from a single, resonance-stabilized free-radical r_1 , whose resonance forms have the odd electron at positions 3, 4a and 6, scheme I. Then oxygenation of r_1 at position 6, favored on steric and electronic grounds, produces monomeric peroxy radical r'_1 .

According to the literature,⁵ propagation steps are expected to include parallel (hydrogen) abstraction and addition reactions, in the present case reactions of r'_1 with 1, to form hydroperoxide monomer 2 and a dimeric radical r_{2a} or r_{2b} , respectively, scheme IIa. These radicals are shown undergoing oxygenation to r'_{2a} and r'_{2b} , leading to dimers and higher oligomers, and homolytic peroxide cleavage producing 3a and 3b from the right sides directly and 4a and 4b from the (identical) left sides in further oxygenation and addition steps, scheme IIb. For the sake of simplicity, 1 is shown as the source of hydrogen in all abstraction steps. Addition of r'_1 to 1 at C₄ leads to radical r_{2a} , which corresponds to 5a, scheme III, the major dimer among several observed using HPLC and FAB MS, see above. No evidence of oligomers with alcohol end groups was found. Alcohol 10 might conceivably form by peroxide cleavage of the oligomer radicals, but HPLC of the autooxidation mixture spiked with 10 showed that its yield in the autooxidation was less than 0.2%.

The other autooxidation products observed using HPLC formed in secondary reactions of 2 and 3a, scheme IV. Dienone 6, the formal dehydration product of 2, appeared in ethylene dichloride solutions of 2 purged with nitrogen or air. In solutions of the mixed epoxides 3a and 3b purged with nitrogen or air, 3a rearranged to 7 while 3b persisted. Compound 7 was further air oxidized to 8 and 9.

The ester side chain and lactone ring of simvastatin 1 were found intact in all of its autooxidation products. The stability of the side chain was confirmed in autooxidation of lovastatin, another Merck cholesterol-lowering agent whose structure differs only by a methyl group (2"-methylbutyryl side chain instead of 2",2"-dimethylbutyryl). Under the same reaction conditions, lovastatin analogues of all the autooxidation products of 1 appeared, and there were no extraneous HPLC peaks. The analogues were readily recognized by their characteristic UV spectra and retention times, that were nearly the same as those of the corresponding products of 1. The reaction rates of 1 and lovastatin in separate kinetic runs were the same, and in a similar run with both 1 and lovastatin present initially, the two disappeared at exactly the same rate.

Free-radical propagation steps are shown in subscripted form with rate expressions in scheme V. Radicals of chain length n are designated r_n , the corresponding peroxy-terminal radicals r'_n , and the oligomeric products P_n . A steady state is pictured in which the parallel abstraction and addition reactions of the r'_n and 1 are rate-determining, fraction X of the monoene-terminal units of the resulting r_{n+1} is cleaved rapidly, and the rest $(1-X)$ is oxygenated. For the sake of simplicity the rate constants and X in scheme V are written as independent of n , and addition to 1 is indicated only at C₄.

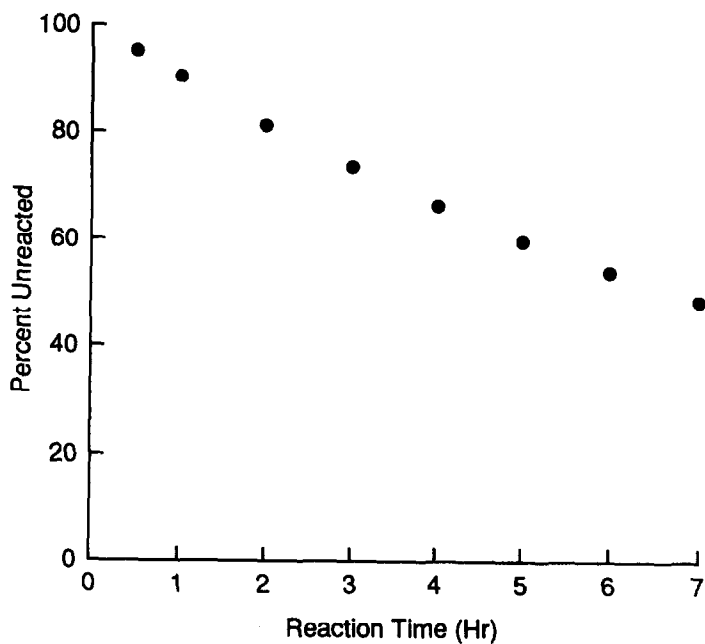


Figure 3. Kinetic data for starting material 1.

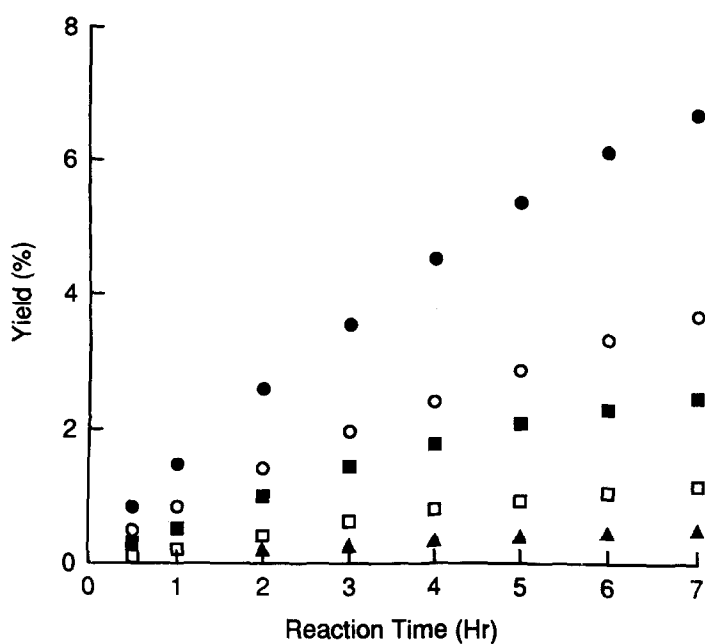


Figure 4. Kinetic data for the oligomers.

Yield = $100 \times (\text{moles of oligomer}) / (\text{initial moles of 1})$.

Key: (●) monomer 2; (○) dimers 5; (■) trimers; (□) tetramers; (▲) pentamers.

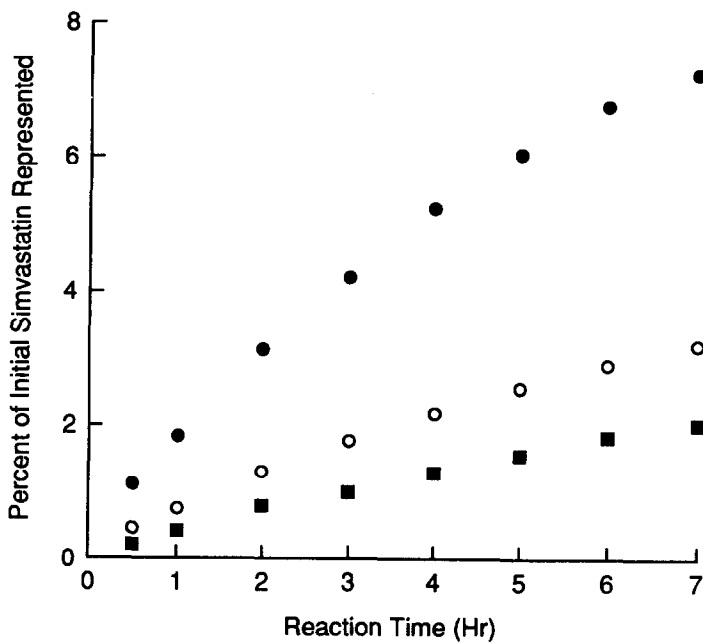


Figure 5. Kinetic data for the epoxides.
Key: (●) 3a; (○) 3b; (■) 4a + 4b.

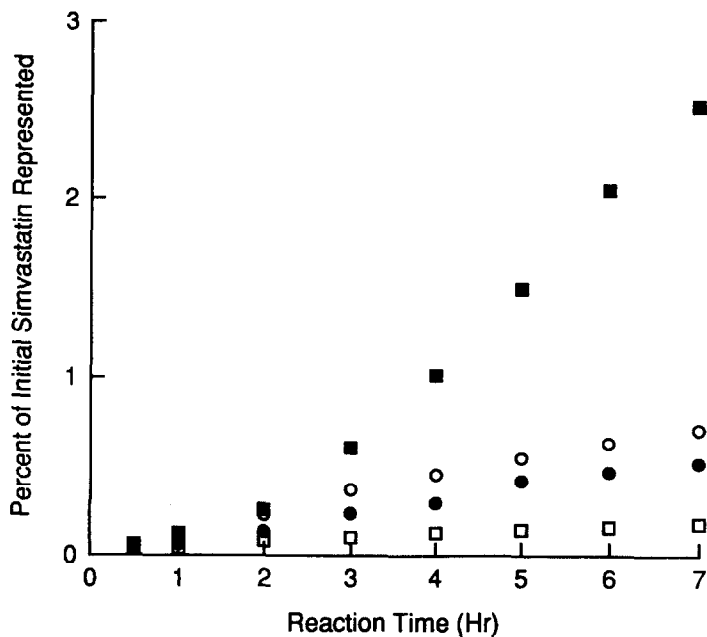
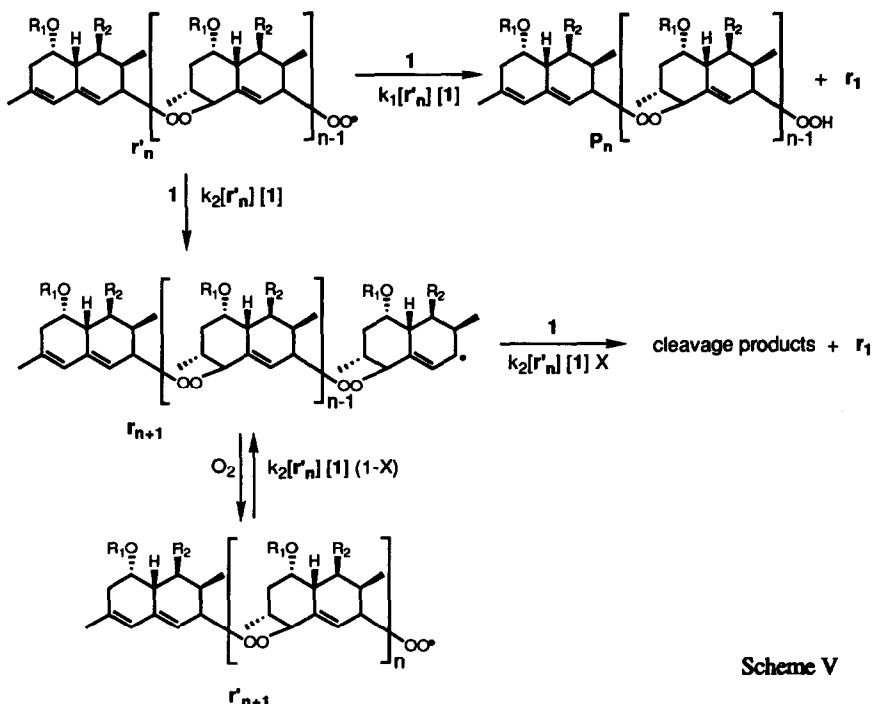


Figure 6. Kinetic data for secondary products.
Key: (●) 6; (○) 7; (■) 8; (□) 9.



Compound **1** is consumed in the abstraction, addition and cleavage steps.

$$-d[1]/dt = [1](k_1 + k_2 + k_2X)\{[r'_1] + [r'_2] + [r'_3] + \dots\} \quad (1)$$

The dependence of the autooxidation rate on the concentrations of the substrate and initiator can be derived as follows.¹ At steady state, the rates of free-radical initiation and termination are equal. First-order decomposition of AMDN is assumed to control the rate of initiation, in which r_1 is produced with efficiency e , and a single rate constant is written for all second-order termination steps, eq. (2).

$$2ek_{\text{ini}}[\text{AMDN}] = 2k_{\text{term}}\{[r'_1] + [r'_2] + [r'_3] + \dots\}^2 \quad (2)$$

By combining eqs. (1) and (2) to eliminate the sum of the $[r'_n]$, the calculated disappearance rate of **1** is found proportional to the concentration of **1** and the square root of the concentration of AMDN.

$$-d[1]/dt = (k_1 + k_2 + k_2X)e^{1/2} (k_{\text{ini}}/k_{\text{term}})^{1/2}[1][\text{AMDN}]^{1/2} \quad (3)$$

Initial disappearance rates of **1** in autooxidations at concentrations of **1** from 10 to 100 mM with AMDN from 0.02 to 0.6 mM conformed to eq. (3). Autooxidations of **1** at concentrations below 10 mM gave rise to a different complex mixture, lacking the familiar oligomers and epoxides, that was not pursued.

According to scheme V the ratios of successive oligomers are determined by the relative concentrations of the r'_n , eq.(4), whose steady state is described by eq.(5).

$$\frac{d[P_{n+1}]/dt}{d[P_n]/dt} = [r'_{n+1}]/[r'_n] \quad (4)$$

$$k_2[r'_n][1](1-X) = (k_1+k_2)[r'_{n+1}][1] \quad (5)$$

By combining eqs.(4) and (5) to eliminate $[r'_{n+1}]$ and $[r'_n]$, the ratios of successive oligomer concentrations are found independent of n .

$$\frac{d[P_{n+1}]/dt}{d[P_n]/dt} = k_2(1-X)/(k_1+k_2) \quad (6)$$

Accordingly, at any given reaction time, $\log [P_n]$ should vary linearly with n . Such a log plot of the oligomer peak areas from Figure 2 (proportional to the oligomer molarities) is nonlinear, however, with steeper slope at higher n , Figure 7. This result suggests that k_1 , k_2 and X may not be independent of n , as assumed, or that cleavage may not be limited to the monoene-terminal linkages. The other linkages seem relatively stable since the slope of the log plot increases only about 1.6-fold over the range of n from 1 to 8. It is reasonable that those linkages are relatively stable since their cleavage would produce diradicals with free electrons insulated from each other.

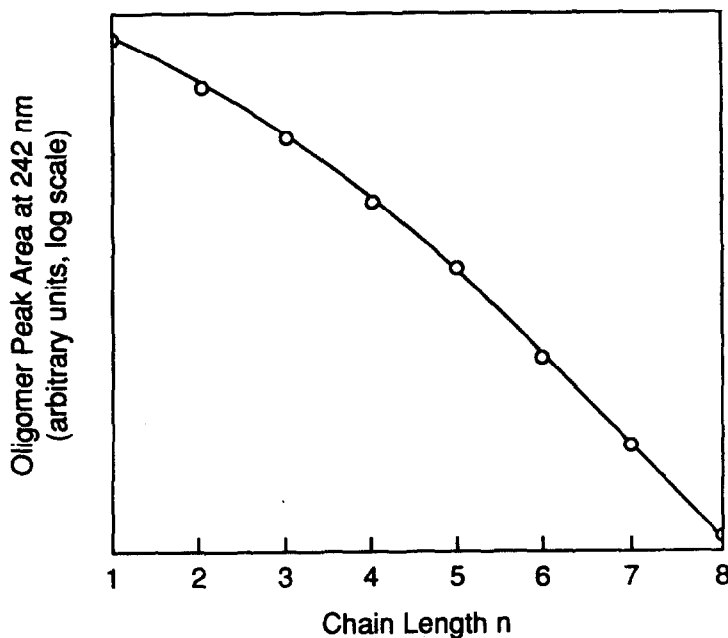


Figure 7. Oligomer composition.

Experimental Section

Materials. Acetonitrile (Fisher HPLC-grade), ethanol USP 200 proof (Quantum Chemical Corp.) and 2,2,4-trimethylpentane (EM Science Omnisolv) were used for HPLC mobile phases. Simvastatin **1**, obtained from the Merck Chemical Manufacturing Division, was aerated in ethylene dichloride, high purity (Burdick and Jackson). Reagents included m-chloroperbenzoic acid, technical grade (Aldrich), sodium borohydride pellets, 98% (Thiokol), and lithium borohydride solution in tetrahydrofuran, (Aldrich).

Autooxidations and Other Reactions. In autooxidation kinetic runs ethylene dichloride solutions of 5-mL volume, containing **1** and a relatively small amount of AMDN, were aerated with a subsurface dry-air stream (20 mL/min) in a flask equipped with a magnetic stirrer, a reflux condenser at -20° to avoid loss of the solvent, and an oil bath to hold the solutions at 35° . Aliquots taken periodically were analyzed using HPLC.

A methylene chloride solution of 0.05 M **1** and 0.07 M m-chloroperbenzoic acid was aged 40 min at room temperature to prepare a mixture of **3a** and **3b**.²⁶ An acetonitrile solution of 0.003 M **2**, isolated from an autooxidation mixture, and equimolar NaBH₄ was aged 2 h at room temperature to make **10**. Compound **11** formed in a tetrahydrofuran solution of 0.003 M **2** and 0.4 M LiBH₄ in 3 h at 40° . HPLC was used to follow these reactions and isolate the products for spectroscopic identification.

High-Performance Liquid Chromatography. Liquid chromatography was performed using a HPLC system composed of an E. Merck-Hitachi model 655A-11 pump, equipped with a ternary gradient controller, and a Hewlett-Packard model 1040A diode array detector, equipped with a HP-85B personal computer, a HP-3390A reporting integrator and a HP-7470A plotter. A 250- X 4.6-mm Partisil PXS 5/25 PAC column (Whatman) was used ordinarily for autooxidation kinetic runs. A mobile phase consisting of 2,2,4-trimethylpentane, absolute ethanol and acetonitrile was delivered at a rate of 2 mL/min, holding the composition 89:7:4 for 16 min, then as a linear gradient to 66:30:4 in 24 min, and finally holding that composition for 10 min, system I. The column was operated at room temperature (23°C), and the effluent was monitored at 210, 242 and 290 nm. A 250- X 4.6-mm Partisil PXS 10/25 PAC column was used also, with a more polar mobile phase consisting of the same solvents, delivered as a linear gradient from 91:5:4 to 50:40:10 in 50 min, system II.

The products were isolated from the autooxidation mixture in milligram amounts for spectroscopic examination using the above columns, a Partisil 10/25 silica column and a semipreparative M9 Partisil 10/50 PAC column with mobile phases consisting of trimethylpentane, ethanol and acetonitrile. Unresolved mixtures of **3a** and **3b** and of **4a** and **4b** served for this purpose. The products were purified to at least 90 area % using HPLC. Then they were dried to constant weight, and the HPLC responses were determined.

NMR Spectroscopy. Samples were prepared in sieve-dried, K₂CO₃-treated CD₂Cl₂. Proton and carbon-13 1-D spectra were recorded on a Bruker WM250 (250.13 MHz ¹H; 62.9 MHz ¹³C) or a Bruker AM400 (400.13 MHz ¹H; 100.61 MHz ¹³C) spectrometer at ambient temperature (23°C). The ¹³C spectrum of **5a** was run at -40°C to sharpen broad resonances obtained at ambient temperature. The chemical shifts are reported in ppm relative to residual CDHCl₂ for proton ($\delta=5.32$ ppm) and relative to CD₂Cl₂ for carbon-13 ($\delta=53.8$ ppm). NMR assignments are footnoted for each structure with carbon-13 data and key proton resonances given. Most of the ¹H assignments are similar to the original simvastatin for which full assignment was made.

Proton multiplicities are abbreviated as follows: s=singlet, d=doublet, t=triplet, m=multiplet, o=overlapping. Spin couplings are in Hz. Grouped shifts and assignments are provided where ambiguities were not resolved. The NOE data was obtained using NOE difference spectroscopy. Carbon multiplicities were determined via the attached proton test (APT) method.²⁷ The 2-D COSY and HETCOR experiments were used to establish regiochemistry and assignments for some compounds. In COSY experiments a data matrix of 1K X 256 with a digital resolution of 4.0-5.0 Hz per point in each dimension was used. A data matrix of 4K X 64 with a digital resolution of 17-20 Hz per point in the f1 dimension and 5-8 Hz per point in the f2 dimension was used in HETCOR experiments.

Mass Spectroscopy. Low-resolution positive-ion FAB measurements were performed with a MAT 731 double focusing magnetic sector mass spectrometer. A Finnigan TSQ 70 quadrupole mass spectrometer was used to obtain negative-ion FAB data. 3-Nitrobenzyl alcohol was used as the matrix for FAB experiments.

High-resolution FAB measurements were performed versus polyethylene glycol with a JEOL HX-110A double focusing magnetic sector mass spectrometer set at a resolution of 5000. The exact mass of (3a+3b) was measured versus perfluorokerosene by high-resolution EI mass spectrometry with a MAT212 mass spectrometer set at a resolution of 5000.

References and Footnotes

1. Miller, A.A.; Mayo, F.R. *J. Amer. Chem. Soc.* **1956**, *78*, 1017-1054.
2. Mayo, F.R. *J. Amer. Chem. Soc.* **1958**, *80*, 2465-2507.
3. *The Chemistry of Peroxides*; Patai, S., Ed.; John Wiley & Sons: New York, 1983; pp 422-428.
4. Cais, R.E.; Bovey, F.A. *Macromolecules* **1977**, *10*, 169-178.
5. Mayo, F.R. *Acc. Chem. Res.* **1968**, *1*, 193-201.
6. Nukui, M.; Yoshino, K.; Ohkatsu, Y.; Tsuruta, T. *Macromolekulare Chemie* **1979**, *180*, 523-526.
7. Budinger, P.A.; Mooney, J.R.; Grasselli, J.G.; Fay, P.S.; Guttman, A.T. *Anal. Chem.* **1981**, *53*, 884-889.
8. Schadel, U.; Neuenschwander, M. *Chimia* **1986**, *40*, 239-241.
9. **1** ¹³C NMR δ 179.3 (C_{1'}), 171.7 (C₆), 134.6 (C₆), 133.4 (C_{4a}), 131.3 (C₄), 130.0 (C₅), 77.9 (C_{2'}), 69.7 (C₁), 64.4 (C₄), 44.6 (C_{2'}), 40.3 (C_{5'}), 39.2 (C_{8a}), 38.4 (C₈), 37.8 (C_{3'}), 34.7, 34.6, 34.4 (C₂, C₁₀, C_{3'}), 32.4 (C₇), 29.1 (C₃), 26.2 (2"-CH₃ (2 C)), 25.9 (C₉), 24.6 (3-CH₃), 15.3 (7-CH₃), 10.9 (C_{4'}); ¹H NMR δ 5.99 (d, J=9.7, H₅), 5.79 (dd, J=9.7, 6.2, H₆), 5.51 (m, H₄), 5.34 (m, H₁), 4.59 (m, H₂), 4.34 (m, H_{4'}), 2.68, 2.55 (dd, J=17.5, 5.0; ddd, J=17.5, 3.7, 1.6, 5'-CH₂), 2.42-2.39 (om, H₃, H₇), 2.29 (m, H_{8a}), 2.10 (br s, 4'-OH), 1.114 (s, 2"-CH₃), 1.108 (s, 2"-CH₃), 1.07 (d, J=7.4, 3-CH₃), 0.89 (d, J=7.0, 7-CH₃), 0.82 (t, J=7.5, 4"-CH₃).
10. **2** ¹³C NMR δ 177.9 (C_{1'}), 171.8 (C₆), 141.2, 134.9 (C₃, C_{4a}), 124.3 (C₄), 117.0 (C₅), 83.4 (C₆), 77.0 (C_{2'}), 67.5 (C₁), 62.8 (C₄), 43.0 (C_{2'}), 41.1 (C_{8a}), 38.3 (C_{5'}), 36.7 (C₂), 34.9 (C_{3'}), 33.2 (C_{3'}), 31.6 (C₁₀), 30.5 (C₈), 30.0 (C₇), 25.7 (C₉), 25.1 (2"-CH₃), 24.3 (2"-CH₃), 23.3 (3-CH₃), 10.1 (7-CH₃), 9.4 (C_{4'}); ¹H NMR δ 9.47 (s, 6-OOH), 5.92 (broad s, H₄), 5.42 (d, J=5.2, H₅), 5.33 (m, H₁), 4.19 (d, J=5.2, H₆), 1.73 (s, 3-CH₃).
11. Bax, A.; Morris, G. A. *J. Mag. Res.* **1981**, *42*, 501-505.
12. van Lier, J.E.; Kan, G. *J. Org. Chem.* **1972**, *37*, 145-147.

13. (a) **10** ^{13}C NMR δ 177.7 (C_1^+), 170.1 (C_6), 137.8, 134.4 (C_3 , C_{4a}), 124.5 (C_4), 123.0 (C_5), 76.4 (C_2), 70.4 (C_6), 67.8 (C_1), 63.3 (C_4), 43.2 (C_2^+), 40.0 (C_{8a}), 39.0 (C_5), 36.5₉, 36.5₇ (C_2 , C_3), 36.1 (C_7), 33.6 (C_{10}), 33.5 (C_3^+), 31.7 (C_8), 25.0₈ (2^--CH_3), 25.0₅ (C_9), 24.5 (2^--CH_3), 23.4 (3-CH_3), 10.8 (7-CH_3), 9.5 (C_4^+); ^1H NMR δ 5.89 (broad d, $J=4.3$, H_5), 5.35 (m, H_1), 3.89 (t, $J=4.3$, H_6), 2.40 (broad d, $J=18.4$, C_2H), 2.21 (dd, $J=18.4$, 2.0, C_2H), 1.71 (s, 3-CH_3), 0.75 (d, $J=7.5$, 7-CH_3). (b) Terahara, A.; Tanaka, M. U.S. Patent 4,517,373, published May 14, 1985.
14. **11** ^{13}C NMR δ 137.3, 134.9 (C_3 , C_{4a}), 124.5 (C_4 , C_5), 72.5, 71.6, 70.5, 65.5 (C_1 , C_6 , C_2 , C_4'), 61.3 (C_6), 43.8, 41.3, 39.8, 39.5, 36.0, 34.6, 30.0, 23.7, 23.6 (C_9), 10.7 (7-CH_3); ^1H NMR δ 5.84 (s, H_4), 5.59 (d, $J=4.8$, H_5), 4.42 (broad s, H_1), 3.89 (d, $J=4.8$, H_6), 2.41 (broad d, $J=16.7$, C_2H), 2.19 (dd, $J=16.7, 1.6$, C_2H), 1.75 (s, 3-CH_3), 0.71 (d, $J=7.1$, 7-CH_3).
15. **5a** ^{13}C NMR (Note: The chemical shifts for the two ester side chains and lactone moieties in this dimer are almost identical so that they are listed under the same numerical assignment) δ 177.5, 177.4 (C_1^+), 172.0, 170.7 (C_6^+), 141.0 (C_{14a}), 140.6, 134.9 (C_3 , C_{4a}), 123.6 (C_4), 122.8 (C_{15}), 116.4 (C_5), 87.5 (C_{14}), 82.3 (C_{16}), 81.2 (C_6), 76.6, 76.0 (C_2), 69.5 (C_{11}), 67.0 (C_1), 62.4, 62.3 (C_4'), 42.7, 42.6 (C_2^+), 39.9 (C_{18a}), 38.9 (C_{8a}), 38.2, 37.9 (C_5), 35.7, 34.4 (C_2 , C_3^+), 33.1, 31.4 (C_{10} , C_{20}), 32.9 (C_3^+), 31.2 (C_8 , C_{12}), 30.4 (C_{13}), 30.0 (C_7), 29.3, 28.7 (C_{17} , C_{18}), 25.2 (C_{19}), 24.9 (2^--CH_3), 24.8 (2^--CH_3), 24.0 (2^--CH_3), 23.8 (2^--CH_3), 24.1 (C_9), 23.3 (3-CH_3), 18.9 (13-CH_3), 9.9 (17-CH_3), 9.7 (7-CH_3), 9.3₄, 9.2₇ (C_4^+), ^1H NMR δ 8.92 (broad s, 16-OOH), 5.90 (s, H_4), 5.79 (d, $J=4.8$, H_{15}), 5.33 (om, H_1 , H_5), 5.31 (m, H_{11}), 1.73 (s, 3-CH_3), 1.02 (d, $J=7.6$, 13-CH_3).
16. (a) **3a** ^{13}C NMR δ 177.4 (C_1^+), 170.1 (C_6), 140.9 (C_6), 128.4 (C_5), 76.3 (C_2), 67.9 (C_1), 66.0 (C_4), 63.0 (C_4'), (C_{4a} unobserved), 43.1 (C_2^+), 39.8, 38.6 (C_8 , C_{8a}), 38.9 (C_5), 36.3 (C_3), 33.4 (C_{10}), 33.0 (C_3^+), 30.3 (C_7), 29.9 (C_2), 27.2 (C_3), 25.3 (C_9), 24.9 (2^--CH_3 (2C)), 19.6 (3-CH_3), 13.7 (7-CH_3), 9.5 (C_4^+); ^1H NMR δ 6.24 (dd, $J=9.6$, 6.2, H_6), 5.12₂ (m, H_1), 5.11₇ (d, $J=9.6$, H_5), 2.97 (s, H_4), 1.33 (d, $J=7.5$, 3-CH_3), 0.93 (d, $J=7.2$, 7-CH_3). (b) **3b** ^{13}C NMR δ 178.6 (C_1^+), 170.1 (C_6), 137.3 (C_4), 129.2 (C_{4a}), 76.5 (C_2), 67.2 (C_1), 63.0 (C_4'), 58.6 (C_6), 55.2 (C_5), 43.3 (C_2^+), 39.1 (C_5), 37.3, 36.6 (C_3), 33.8, 33.5 (C_2 , C_{10}), 33.2 (C_3^+), 31.0, 29.6 (C_8 , C_{8a}), 27.9 (C_3), 24.8 (2^--CH_3 (2C)), 24.2 (C_9), 22.9 (3-CH_3), 9.5 (C_4^+), 9.4 (7-CH_3); ^1H NMR δ 5.91 (m, H_4), 5.23 (m, H_1), 3.35 (d, $J=4.0$, H_5), 3.28 (m, H_6), 1.13 (d, $J=7.5$, 3-CH_3), 0.78 (d, $J=6.9$, 7-CH_3).
17. *Applications of Nuclear Magnetic Resonance in Organic Chemistry*; Jackman, L. M.; Sternhell, S.; Ed.; Pergamon Press: Oxford, 1969; pp 227-229.
18. *Carbon-13 NMR Spectroscopy*; Kalinowski, H. O.; Berger, S.; Braum, S.; Ed.; John Wiley & Sons: New York, 1988; pp 346-352, 499.
19. (a) **4a** ^{13}C NMR δ 177.5 (C_1^+), 170.2 (C_6), 136.0 (C_{4a}), 133.5 (C_4), 81.0 (C_3), 76.3 (C_2), 69.5 (C_1), 62.9 (C_4'), 58.4 (C_6), 54.3 (C_5), 43.1 (C_2^+), 38.7 (C_5), 37.0 (C_{8a}), 36.1 (C_3), 35.7 (C_2), 33.2 (C_3^+), 32.7 (C_{10}), 30.5 (C_8), 29.0 (C_7), 26.0 (3-CH_3), 24.8 (2^--CH_3), 24.7 (2^--CH_3), 23.7 (C_9), 9.4₄ (C_4^+), 9.2 (7-CH_3); ^1H NMR δ 7.65 (s, 3-OOH), 5.98 (m, H_4), 4.99 (m, H_1), 3.39 (d, $J=4.0$, H_5), 3.31 (m, H_6), 1.28 (s, 3-CH_3), 0.91 (d, $J=7.1$, 7-CH_3). (b) **4b** ^{13}C NMR δ 178.2 (C_1^+), 170.2 (C_6), 134.7 (C_{4a}), 132.4 (C_4), 79.8 (C_3), 76.2 (C_2), 66.4 (C_1), 62.9 (C_4'), 58.3 (C_6), 54.2 (C_5), 43.1 (C_2^+), 38.7 (C_5), 37.5 (C_{8a}), 36.7 (C_2), 36.2 (C_3), 33.1 (C_3^+), 32.8 (C_{10}), 30.2 (C_8), 29.2 (C_7), 25.6 (3-CH_3), 24.6 (2^--CH_3), 24.5 (2^--CH_3), 24.0 (C_9), 9.3₉ (C_4^+), 9.2 (7-CH_3); ^1H NMR δ 7.52 (s, 3-OOH), 5.99 (m, H_4), 5.36 (m, H_1), 3.39 (d, $J=4.0$, H_5), 3.31 (m, H_6), 1.34 (s, 3-CH_3), 0.92 (d, $J=7.0$, 7-CH_3).
20. **6** ^{13}C NMR δ 203.4 (C_6), 177.4 (C_1^+), 170.2 (C_6), 154.9 (C_{4a}), 144.4 (C_3), 124.2, 122.8 (C_4 , C_5), 75.8 (C_2), 66.6 (C_1), 62.9 (C_4'), 43.1 (C_2^+), 42.4 (C_7), 39.2 (C_{8a}), 38.6 (C_5), 37.4 (C_8), 36.4, 36.1 (C_2 , C_3), 33.2 (C_3^+), 32.5 (C_{10}), 24.8 (2^--CH_3), 24.2 (2^--CH_3), 24.0 (C_9 , 3-CH_3), 10.4 (7-CH_3), 9.4 (C_4^+); ^1H NMR δ 6.13 (broad s, H_4), 5.71 (broad s, H_5), 5.38 (m, H_1), 1.84 (s, 3-CH_3), 0.99 (d, $J=7.4$, 7-CH_3).
21. Joshua, H.; Schwartz, M. S.; Wilson, K. E. *J. Antibiot* **1991**, *44*, 366-370.
22. **7** ^1H NMR δ 6.16 (dd, $J=9.7$, 3.3, H_6), 5.57 (d, $J=9.7$, H_5), 5.52 (m, H_1), 3.71 (d, $J=7.2$, H_4).
23. (a) Aue, W. P.; Bartholde, E.; Ernst, R. R. *J. Chem. Phys.* **1976**, *64*, 2229-2246. (b) Nagayama, K.; Kumar, A.; Wuthrich, K.; Ernst, R. R. *J. Mag. Res.* **1980**, *40*, 321-334.
24. **8** ^{13}C NMR δ 177.5 (C_1^+), 170.1 (C_6), 139.6, 139.4, 136.5, 132.2 (C_{4a} , C_7 , C_8 , C_{8a}), 131.4 (C_6), 125.4 (C_5), 75.6 (C_2), 73.8 (C_4), 67.8 (C_1), 63.3 (C_4'), 42.9 (C_2^+), 38.9 (C_5), 35.8₈ (C_3), 35.8₅ (C_{10}), 34.6 (C_3), 33.4 (C_3^+), 33.0 (C_2), 24.8 (2^--CH_3), 24.6 (2^--CH_3), 24.1 (C_9), 19.9 (7-CH_3), 19.2 (3-CH_3), 9.4 (C_4^+); ^1H NMR δ 7.28 (d, $J=7.9$, H_5), 7.19 (d, $J=7.9$, H_6), 6.15 (dd, $J=5.6, 3.2$, H_1), 4.48 (d, $J=6.3$, H_4), 2.33 (s, 7-CH_3), 1.13 (d, $J=7.0$, 3-CH_3).

25. ^2H NMR δ 7.90 (d, $J=7.9$, H₅), 7.33 (d, $J=7.9$, H₆), 6.34 (t, $J=4.0$, H₁), 2.44 (s, 7-CH₃), 1.40 (d, $J=7.5$, 3-CH₃).
26. *Reagents for Organic Synthesis*; Fieser, M.; Fieser, L. F.; Ed.; John Wiley & Sons: New York, 1967; Vol. 1 pp 136-137.
27. Patt, S. L.; Schoolery, J. H. *J. Mag. Res.* 1982, 46, 535-539.

Acknowledgments

The authors thank Drs. E. J. J. Grabowski, M.J. Kaufman and S.G. Mills for helpful discussions, Mr. J.L. Smith for part of the mass spectroscopy and Mrs. H.R. Graham for manuscript preparation. The authors also thank one of the referees for noting the likely addition of radical r'_1 to I at C₆ as well as C₄, as shown in scheme IIa.